Send Orders for Reprints to reprints@benthamscience.net

Current Alzheimer Research, 2022, *19*, 618-627

RESEARCH ARTICLE

Distribution of Cortical Atrophy Associated with Cognitive Decline in Alzheimer's Disease: A Cross-Sectional Quantitative Structural MRI Study from PUMCH Dementia Cohort

Chenhui Mao[1,#], Bo Hou[2,#], Jie Li[1], Shanshan Chu[1], Xinying Huang[1], Jie Wang[1], Liling Dong[1], Caiyan Liu[1], Feng Feng[2,*], Bin Peng[1] and Jing Gao[1,*]

[1]*Department of Neurology, State Key Laboratory of Complex Severe and Rare Diseases, Peking Union Medical College Hospital, Chinese Academy of Medical Science/Peking Union Medical College, Beijing 100730, China;* [2]*Department of Radiology, Peking Union Medical College Hospital, Chinese Academy of Medical Science/Peking Union Medical College, Beijing 100730, China*

ARTICLE HISTORY

Received: March 05, 2022
Revised: June 25, 2022
Accepted: June 28, 2022

DOI:
10.2174/1567205019666220905145756

Abstract: ***Background*:** Quantitative measures of atrophy on structural MRI are sensitive to the neurodegeneration that occurs in AD, and the topographical pattern of atrophy could serve as a sensitive and specific biomarker.

***Objective*:** We aimed to examine the distribution of cortical atrophy associated with cognitive decline and disease stage based on quantitative structural MRI analysis in a Chinese cohort to inform clinical diagnosis and follow-up of AD patients.

***Methods*:** One hundred and eleven patients who were clinically diagnosed with probable AD were enrolled. All patients completed a systemic cognitive evaluation and domain-specific batteries. The severity of cognitive decline was defined by MMSE score: 1-10 severe, 11-20 moderate, and 21-30 mild. Cortical volume and thickness determined using 3D-T1 MRI data were analyzed using voxel-based morphometry and surface-based analysis supported by the DR. Brain Platform.

***Results*:** The male:female ratio was 38:73. The average age was 70.8 ± 10.6 years. The mild: moderate: severe ratio was 48:38:25. Total grey matter volume was significantly related to cognition while the relationship between white matter volume and cognition did not reach statistical significance. The volume of the temporal-parietal-occipital cortex was most strongly associated with cognitive decline in group analysis, while the hippocampus and entorhinal area had a less significant association with cognitive decline. Volume of subcortical grey matter was also associated with cognition. Volume and thickness of temporoparietal cortexes were significantly correlated with the cognitive decline, with a left predominance observed.

***Conclusion*:** Cognitive deterioration was associated with cortical atrophy. Volume and thickness of the left temporal-parietal-occipital cortex were most important in early diagnosis and longitudinal evaluation of AD in clinical practice. Cognitively relevant cortices were left predominant.

Keywords: Alzheimer's disease, cortical thickness, cortical volume, cognitive decline, structure MRI, quantitative.

1. INTRODUCTION

Alzheimer's disease (AD) is the most common neurodegenerative dementia causing progressive brain atrophy and cognitive impairment. Although the existing, extensive research has revealed the possible pathogenesis and mechanism of AD, we still had no effective disease-modifying treatment for the disease [1]. The characteristic features of Alzheimer's pathology are amyloid plaques and neurofibrillary tangles (NFTs). In addition, neuropil threads, dystrophic neurites, astrogliosis and microglial activation, progressive neuronal loss, as well as cortical vacuolation, are seen [2]. The most prevalent theory of AD pathogenesis is the amyloid cascade hypothesis that posits an accumulation of pathological Aβ causes the formation of neurofibrillary tangles and subsequent neurodegeneration and neuronal dysfunction [3]. It is well-known that the pathogenesis and pathological protein accumulation precede clinical cognitive impairment,

*Address correspondence to these authors at the Department of Neurology, State Key Laboratory of Complex Severe and Rare Diseases, Peking Union Medical College Hospital, Chinese Academy of Medical Science/ Peking Union Medical College, Shuaifuyuan 1st, Dongcheng District, Beijing 100730, China; E-mail: gj107@163.com (J.G.); Department of Radiology, Peking Union Medical College Hospital, Chinese Academy of Medical Science/Peking Union Medical College, Shuaifuyuan 1st, Dongcheng District, Beijing 100730, China. E-mail: cjr.fengfeng@vip.163.com (F.F.)

#*The two authors contributed equally to this work.*

Current Alzheimer Research

1875-5828/22 $65.00+.00 © 2022 Bentham Science Publishers

therefore, biomarkers are important in detecting pre-symptom and early-stage AD patients [4].

The most common presentation of AD is the insidious onset and progressive loss of episodic memory in an elderly individual. As the condition progresses, cognitive difficulties become more profound and widespread, interfering with activities of daily living and social functioning [5]. However, there are also atypical syndromes in AD, including posterior cortical atrophy, logopenic aphasia and the frontal variant. Posterior cortical atrophy patients typically present with prominent and early visuospatial and visual perceptual problems [6]. Logepenic aphasia patients present with prominent word-finding pauses and anomia [7]. Frontal AD patients present with executive dysfunction, abnormal behavior and neuropsychiatric symptoms resembling the behavioral variant of frontotemporal dementia [8]. The clinical diagnosis of AD is based on clinical presentation, a neuropsychiatry battery evaluation and exploration of a differential diagnosis, as illustrated both in 1984 NINCDS-ADRDA criteria [9] and in 2011 NIA-AA criteria [10]. The MRI is included in both criteria and is useful for excluding other diseases.

Although not specific to AD pathology, atrophy on structural MRI is widely used in the clinical diagnosis and research of AD. The typical patterns of atrophy, including temporal lobe and fronto-temporo-parietal neocortex atrophy, inform AD diagnosis [11]. Also, atrophy of the medial temporal structures, especially the hippocampus, could be a predictor of MCI conversion to AD [12]. Thus, several visual rating scales have been created to semi-quantitatively evaluate brain atrophy in the clinical diagnosis of AD. The medial temporal atrophy [MTA] scale is a classical and widely used tool in AD MRI evaluation [13]. Later on, the visual assessment of posterior atrophy and a comprehensive visual rating scale was introduced by different researchers to facilitate AD clinical diagnosis using a structural MRI [14, 15]. In 2018, the NIA-AA research framework defined AD using biomarkers irrelevant to clinical cognitive status. The atrophy of the cortex shown by a structural MRI was incorporated as a neurodegenerative biomarker, along with CSF t-tau elevation and FDG-PET hypo-metabolism [16]. Compared with lumber puncture and FDG-PET, MRI is completely noninvasive and widely available.

However, the atrophy pattern of AD was affected by age-onset, genetic background, and clinical subtype. In an early onset AD, atrophy of the posterior cortex, including the precuneus, is more prominent, while medial temporal cortex atrophy is usually found in late-onset AD [17]. Scahill *et al.* also found APP subjects exhibited more medial temporal lobe atrophy and memory deficits, while PSEN1 subjects showed more neocortical loss and greater impairment in non-memory domains [18]. The atrophy patterns in the different clinical subtypes of AD are different. In logopenic aphasia, predominant left posterior perisylvian or parietal atrophy is found [19]. Cross-sectional voxel-based morphometry research revealed the most significant atrophy found in regions of the occipital and parietal lobes in posterior cortical atrophy [20].

Manual or visual methods for the detection of atrophy in AD could only focus on a few selected regions, such as the hippocampus or entorhinal cortex, which is far from supporting an early and precise diagnosis. The introduction of computer-based methods for quantitative MRI has allowed for efficient quantification of cortical atrophy [21, 22]. This further emphasized that even pre-symptomatic AD was associated with atrophy of the temporal, inferior parietal and posterior cingulate [23, 24]. The degree of clinical impairment is associated with the severity of atrophy [25]. So quantitative structural MRI was sensitive in early diagnosis of AD and was predictive of decline to dementia in individuals with mild cognitive impairment [26]. In this article, we aimed to verify the distribution of cortical atrophy associated with cognitive decline and disease stage based on quantitative structure MRI analysis in a Chinese cohort. We hoped the findings of this article would help clinicians focus on specific brain regions in the diagnosis and disease monitoring of AD, to better incorporate MRI into clinical diagnosis and follow-up of AD patients.

2. MATERIALS AND METHODS

2.1. Subjects Inclusion

This was a cross-sectional observational study. Patients in this study were recruited from the dementia clinic database, department of neurology in Peking Union Medical College Hospital (PUMCH-dementia cohort), north China. The study was conducted according to the Declaration of Helsinki in 1975. All patients or their caregivers were informed regarding the purpose of the study and the publishing of the article. Written consent was obtained from each patient or their caregiver(s). Peking Union Medical College Hospital's ethics committee approved the study (No. JS2810].

A total of 111 AD patients were enrolled. Inclusion criteria were in accordance with the probable Alzheimer's disease criteria in 2011 NIA-AA guideline [10]. Detailed clinical information, including symptoms onset and progression was provided by reliable informants. All patients underwent a systemic physical examination, laboratory blood tests (including hepatic function, renal function, homocysteine, thyroid function, folic acid, vitamin B12, blood ammonia and rapid plasma regain test) and neuroimaging that were necessary for diagnosis and differential diagnosis [27]. Besides, we analyzed the genotype of apolipoprotein E (ApoE) [28].

2.2. Neuropsychological Assessment

Detailed cognition battery included screening tests: Mini-Mental State Examination (MMSE), Montreal Cognitive Assessment-PUMCH edition (MoCA-PUMCH edition) [28], Activities of Daily Living (ADLs) and Hospital Anxiety and Depression Scale (HADS). After screening, a detailed domain-specific battery was conducted, including story memory, category fluency, Trail Making A and B, digit symbol, digit span, auditory verbal learning test, block design test and modified Rey figure, among others. All these chosen scales were validated in Mandarin e with available normative data for the Chinese population.

2.3. Structure MRI Data Acquisition

MRI examinations were performed using a 3-T MRI scanner (Discovery MR750 3 T, GE Healthcare, Milwaukee,

WI, USA). Thirty-two channel head coils were used. Axial T1-weighted, T2-weighted, fluid-attenuated inversion recovery (FLAIR) and susceptibility weighted imaging (SWI) were performed. Parameters for 3D-T1: Field strength 3T; Plane sagittal; Mode 3D; Pulse sequence BRAVO; Repetition time/echo time (TR/TE) = 7.4/2.8 ms; Resolution=1.0×1.0×1.0 mm; flip angle = 12°; acquisition time (TA) = 6 min 35 s.

2.4. Measurements of Volume and Thickness of Cortex

Data pre-processing and analysis were performed using the Dr. Brain Platform (YiWei Medical Technology Co. Ltd., Shenzhen, China). The volume analysis was based on voxel-based morphometry (VBM) [29, 30]. The data preprocessing involved visual inspection of the T1-weighted images to control for imaging artifacts. Then, bias correction and noise reduction were performed, followed by spatial normalization of each participant's high-resolution 3D T1-weighted scan into the same stereotaxic space to establish voxel for voxel correspondence. This non-linear registration process created a de-formatted image. Then the gray matter, white matter and cerebrospinal fluid were segmented in each image. Individual GM and WM images were spatially smoothed with an isotropic Gaussian kernel approach before entering them into statistical analyses. We used voxel-wise parametric tests to compare the normalized data between the two groups and then multiple comparison correction was performed. The Cortical thickness measurement was based on surface-based analysis (SBA) [30]. Next, surface extraction was performed to mark the surface boundary between cortical white matter and l gray matter as well as the boundary between the gray matter and dura and/or CSF. The cortical thickness was defined as the distance between the two boundaries and was used for group analysis. The control images of cognitively normal participants were obtained from the Dr. Brain Platform. The segmented cortical regions are listed in Supplementary Table **S1**.

2.5. Statistical Analysis

Statistical analyses were performed using SPSS V.25.0 software. The measurement data were described as average ± standard deviation (x ± sd), and count data were described as ratios. Measurement data were statistically analyzed with t-test (two groups) and ANOVA (3 groups), while count data were analyzed using $\chi 2$ test. The level of statistical significance was set to $p<0.05$. Pearson's correlation was used to compare the relationship between cortical atrophy and cognition.

3. RESULTS

3.1. General Characteristics of the Subjects

A total of 111 patients were enrolled in the study. The ratio of male to female patients was 38:73. The age at the time of examination ranged from 41-86 years (70.8 ± 10.6 years). The number of ApoE ε4 carriers was 49 and that of non-carriers was 50, while the remaining 12 patients did not have this information available. MMSE score ranged from 2-30 (17.7 ± 7.9), and MoCA score ranged from 1-27 (15.8 ± 6.9).

3.2. Cognition & Cortical Volume

3.2.1. MMSE Subgroup Analysis

The patients were divided into three cognitive status groups based on MMSE score (mild: MMSE 21-30; moderate: MMSE 11-20; severe: MMSE 0-10).The demographic and clinical information are listed in Table **1**. Age was significantly lower in the severe group. One-way ANOVA was performed to evaluate volume differences in specific cortical and subcortical structures among the three cognitive status groups.

Along with cognitive decline, the most significantly atrophied cortices included the bilateral middle frontal gyrus, middle temporal gyrus, inferior temporal gyrus, superior parietal lobule, supramarginal gyrus, precuneus, angular gyrus, superior occipital gyrus, middle occipital gyrus, inferior occipital gyrus, posterior cingulate gyrus and left superior temporal gyrus ($p<0.0001$) (Table **1**). The hippocampus and entorhinal area were also significantly atrophied with cognitive decline ($p<0.05$) (Supplementary Table **S2**).

Total grey matter volume declined significantly with cognitive decline, while white matter and lateral ventricle volume did not. The volumes of subcortical structure, including caudate, putamen, amygdala and thalamus, were all significantly atrophied with cognitive decline (Table **1**).

3.2.2. Pearson Correlation Analysis

Pearson correlation analysis was performed to evaluate the relationship between volumes of specific structures and global cognition scores on the MMSE and MoCA, respectively. Most atrophied cortical regions correlated with a lower MMSE score (Pearson coefficient>0.5), including left middle temporal gyrus, left inferior temporal gyrus, left supramarginal gyrus, left angular gyrus, left middle occipital gyrus, right middle temporal gyrus, left precuneus, right supramarginal gyrus, left inferior occipital gyrus, and right inferior temporal gyrus (Figs. **1A-F**).

Most atrophied cortical regions correlated with a lower MoCA score (Pearson coefficient>0.5), including the left inferior temporal gyrus, left middle temporal gyrus, left angular gyrus, left supramarginal gyrus, right supramarginal gyrus, right middle temporal gyrus, right middle occipital gyrus, right angular gyrus, left middle occipital gyrus, left inferior occipital gyrus, right inferior temporal gyrus, and left superior parietal lobule (Figs. **1G-L**).

3.3. Cognition & Cortical Thickness

Pearson correlation analysis between cortical thickness and cognitive evaluation revealed that most atrophied cortical regions correlated with a lower MMSE score (Pearson coefficient>0.5), including the left precuneus, left inferior parietal lobule, left isthmus cingulate gyrus, left supramarginal gyrus, right precuneus, left superior parietal lobule, right supramarginal gyrus, and right inferior parietal lobule (Figs. **2A-E**).

Most atrophied cortical regions correlated with a lower MoCA score (Pearson coefficient>0.5), including the left precuneus, left inferior parietal lobule, left supramarginal gyrus, left middle temporal gyrus, left isthmus cingulate gy-

Table 1. Brain structure volume comparison between different cognitive statuses.

Groups	Mild	Moderate	Severe	*p*
No.	48	38	25	-
MMSE ($\bar{x} \pm s$)	25.2 ± 2.6	15.6 ± 2.9	6.4 ± 2.7	-
Sex (Male: Female)	18:30	13:25	7:18	0.719
Age ($\bar{x} \pm s$)	73.5 ± 8.7	70.2 ± 11.2	66.5 ± 11.5	0.023
ApoEε4 carrier: non-carrier	25:20	15:17	9:13	0.497
Cortical Volume, mm^3 ($\bar{x} \pm s$)				
Left Middle Frontal Gyrus	15320.0 ± 1671.1	14199.6 ± 1969.2	12972.0 ± 1822.3	<0.0001
Right Middle Frontal Gyrus	14971.3 ± 1643.1	13633.6 ± 1948.5	13096.9 ± 1974.6	<0.0001
Left Superior Temporal Gyrus	5354.9 ± 743.0	4888.8 ± 746.2	4358.1 ± 720.7	<0.0001
Left Middle Temporal Gyrus	11873.8 ± 1586.2	10504.5 ± 1416.0	9071.5 ± 1446.2	<0.0001
Right Middle Temporal Gyrus	12136.6 ± 1517.6	10707.5 ± 1935.5	9672.2 ± 1580.9	<0.0001
Left Inferior Temporal Gyrus	8750.4 ± 1061.3	7811.2 ± 1229.1	6882.5 ± 1101.2	<0.0001
Right Inferior Temporal Gyrus	9330.4 ± 1185.6	8437.2 ± 1387.3	7667.1 ± 1213.4	<0.0001
Left Superior Parietal Lobule	8663.0 ± 1014.7	7873.0 ± 1098.2	7065.6 ± 1467.5	<0.0001
Right Superior Parietal Lobule	8533.1 ± 912.2	7858.9 ± 1102.9	7227.1 ± 1152.8	<0.0001
Left Supramarginal Gyrus	6889.2 ± 943.2	6184.0 ± 839.7	5264.1 ± 1033.5	<0.0001
Right Supramarginal Gyrus	6258.8 ± 771.3	5563.0 ± 1059.8	4852.8 ± 1005.5	<0.0001
Left Precuneus	9329.7 ± 903.5	8487.9 ± 1306.0	7598.5 ± 1071.6	<0.0001
Right Precuneus	9879.7 ± 1019.8	8747.2 ± 1408.7	8078.0 ± 1358.1	<0.0001
Left Angular Gyrus	7662.6 ± 870.7	6817.2 ± 1194.1	5805.4 ± 1206.7	<0.0001
Right Angular Gyrus	9181.3 ± 1108.5	7953.1 ± 1605.5	7190.8 ± 1503.5	<0.0001
Left Superior Occipital Gyrus	2491.9 ± 342.8	2361.4 ± 469.1	1975.9 ± 515.0	<0.0001
Right Superior Occipital Gyrus	3355.8 ± 565.3	3084.6 ± 537.1	2690.2 ± 573.1	<0.0001
Left Middle Occipital Gyrus	5079.3 ± 633.8	4742.8 ± 722.9	3868.3 ± 798.3	<0.0001
Right Middle Occipital Gyrus	4001.2 ± 476.5	3525.0 ± 647.6	3182.6 ± 585.4	<0.0001
Left Inferior Occipital Gyrus	5220.9 ± 705.5	4700.7 ± 818.3	4010.7 ± 879.4	<0.0001
Right Inferior Occipital Gyrus	5379.6 ± 700.3	4957.5 ± 792.3	4384.0 ± 865.7	<0.0001
Left Posterior Cingulate Gyrus	3364.7 ± 397.9	3028.5 ± 477.2	2816.3 ± 385.5	<0.0001
Right Posterior Cingulate Gyrus	3071.3 ± 360.3	2779.2 ± 468.7	2612.0 ± 381.9	<0.0001
Total Volume, mm^3($\bar{x} \pm s$)				
Total Grey Matter	549374.0 ± 46229.6	514909.0 ± 50169.4	488812.2 ± 45373.0	<0.0001
Total White Matter	435153.6 ± 53052.6	422331.1 ± 51959.1	423894.8 ± 44894.2	0.4574
Left Lateral Ventricle	16158.0 ± 6394.4	17114.4 ± 7295.8	18657.7 ± 6048.6	0.3155
Right Lateral Ventricle	13326.4 ± 5463.3	14197.8 ± 6305.2	14726.0 ± 4978.3	0.5722

(Table 1) Contd…..

Groups	Mild	Moderate	Severe	*p*
Subcortical Volume, mm^3($\bar{x} \pm s$)				
Right Caudate	2397.6 ± 419.8	2134.4 ± 468.7	2029.5 ± 364.1	0.0009
Left Caudate	2183.9 ± 469.7	1997.0 ± 260.9	1867.0 ± 313.2	0.0024
Left Amygdala	656.8 ± 149.6	598.8 ± 125.8	538.4 ± 132.0	0.0027
Right Amygdala	636.7 ± 131.9	597.9 ± 133.0	544.4 ± 114.2	0.0163
Left Putamen	2943.6 ± 461.0	2773.5 ± 459.1	2618.6 ± 600.1	0.0273
Left Thalamus Proper	4215.2 ± 741.5	3829.1 ± 696.3	3854.0 ± 802.3	0.0329
Right Thalamus Proper	4192.3 ± 739.8	3828.0 ± 736.1	3832.2 ± 815.2	0.0475
Right Putamen	2904.7 ± 457.3	2705.2 ± 525.8	2616.9 ± 576.8	0.0485

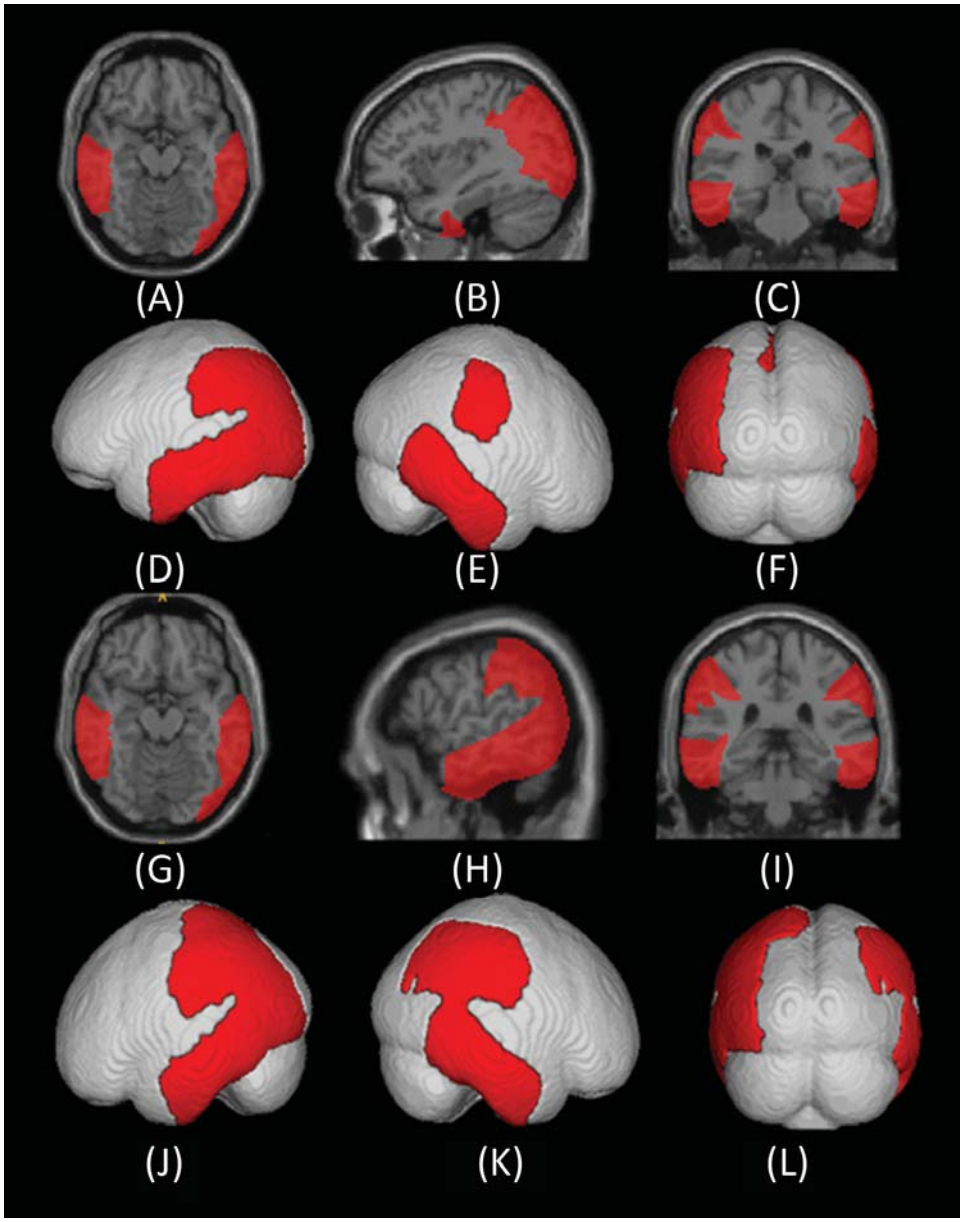


Fig. (1). Results of Pearson correlation analysis between cortical volume and cognitive test score. Red regions represent the most atrophied cortical regions correlated with MMSE (**A-F**) and MoCA (**G-L**) scores (Pearson coefficient>0.5). *(A higher resolution / colour version of this figure is available in the electronic copy of the article).*

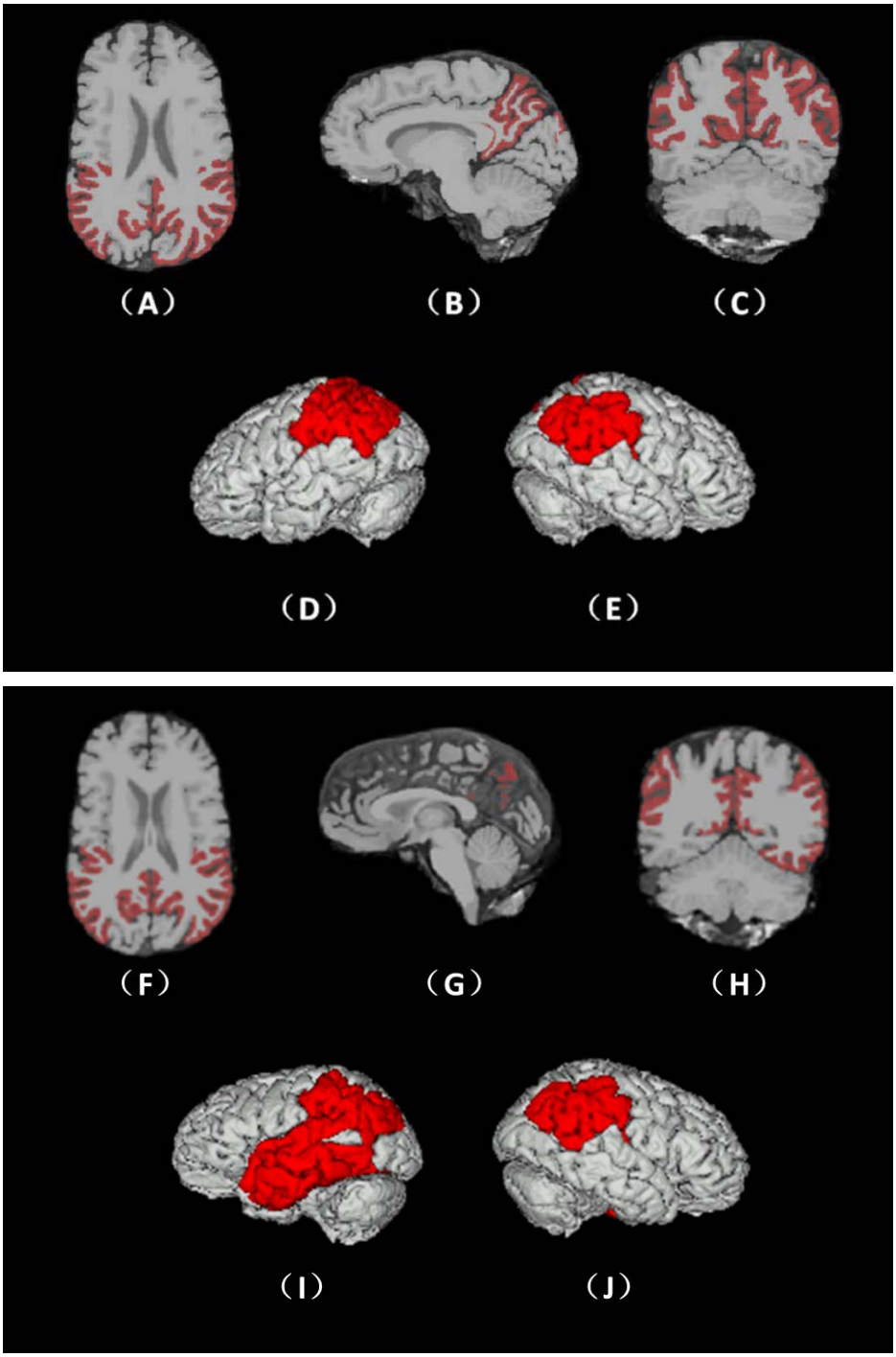


Fig. (2). Results of Pearson correlation analysis comparing cortical thickness and cognitive test score. Red regions represent the most atrophied cortical regions that were significantly correlated with lower MMSE (**A-E**) and MoCA (**F-J**) scores (Pearson coefficient>0.5). *(A higher resolution / colour version of this figure is available in the electronic copy of the article).*

rus, left superior temporal gyrus, left fusiform gyrus, right precuneus, left inferior temporal gyrus, right isthmus cingulate gyrus, right supramarginal gyrus, and right inferior parietal lobule (Figs. **2F-J**).

4. DISCUSSION

Atrophy of the brain is related to cognitive decline in AD progression and MCI conversion to AD. VBM-based research demonstrates that memory function was significantly associated with atrophy of the medial temporal lobe, including the hippocampus, in AD and aMCI [31]. Additionally, baseline volumes of the whole brain, ventricles, hippocampus, and entorhinal cortex are significant predictors of earlier conversion from MCI to AD [32]. Heterogeneous atrophy patterns are found in AD, including limbic predominant, hippocampal sparing and diffuse atrophy subtypes, while

hippocampal sparing and diffuse atrophy subtypes showed worse cognition and more rapid progression [33]. Also, an increased hippocampal volume to cortical volume ratio is predictive of faster clinical decline in AD [34]. In prodromal AD, medial-temporal predominant atrophy is associated with worse memory and language function, and parieto-occipital atrophy is associated with poor executive/attention and visuospatial function [35]. The comparisons between late- and early-onset AD patients reveal more pronounced atrophy of the precuneus in early-onset AD patients and more severe atrophy in the medial temporal lobe in late-onset AD patients [36]. Specific brain region atrophy, including atrophy in the posterior cingulate and precuneus, basal forebrain could help with the early diagnosis of AD [37, 38]. In the current study, the lower temporal-parietal-occipital cortex volume, the precuneus and posterior cingulate volume, and total grey matter volume were most significantly correlated with worse cognitive performance, suggesting the neocortical atrophy is more helpful in diagnosing and monitoring AD. Hippocampus and entorhinal area atrophy was also correlated with worse cognitive performance, but not as strongly as with the neocortex.

The Cortical thickness is a cardinal sign of neurodegeneration and is correlated with the severity of cognitive impairment.The cortical thickness in regions including the entorhinal cortex, temporopolar cortex, lateral temporal cortex, inferior parietal cortex, inferior parietal sulcus, posterior cingulate cortex, and inferior frontal cortex was more sensitive for diagnosis in early and pre-symptomatic AD than hippocampus volume [39]. The cortical thickness analysis also revealed the precuneus and inferior temporal regions were relatively preserved against age-related cortical thinning and AD continuum patients showed a decreased cortical thickness in the perisylvian region [40].The longitudinal research has shown that AD subjects with a thinner entorhinal cortex thickness had lower baseline cognitive scores and greater subsequent cognitive decline at follow-up [41]. Our research also showed cortical thickness in the perisylvian region, including the parietal lobe and lateral temporal lobe was most strongly correlated with the cognitive profile in AD patients. The results were similar to those of cortical volume analysis, indicating that in symptomatic AD patients both cortical volume and thickness are sensitive biomarkers of disease progression.

Cortical atrophy revealed by MRI was correlated with the neuropathological basis of AD. The main neuropathological substrate was neuronal loss and synaptic loss [2]. The underlying mechanism of neuronal loss is complicated, and it was reported that the regional patterns of neuronal loss matched that of NFTs, however, neuronal and synaptic losses were better correlates of cognitive deficits than the number of NFTs [42]. The topographical distribution of cortical atrophy on MRI varied, although the neurofibrillary degeneration started in the allocortex of the medial temporal lobe and spread to the associative neocortex with disease progression [43]. Furthermore, observations from several studies have suggested that this pattern of pathological progression might not be the only pattern of neurofibrillary degeneration [44]. Brain bank-based research has also shown that AD has distinct clinicopathological subtypes, including typical, hippocampal sparing, or predominant limbic subtypes. Hippocampal sparing and limbic-predominant AD subtypes account for about 25% of cases [45]. Although different clinical and pathological subtypes have been demonstrated in AD, Whitwell *et al.* Reported that temporoparietal atrophy is a useful marker of the presence of AD pathology even in subjects with atypical clinical presentations [46]. Our study did not categorize the patients based on clinical presentations. We believe our results support the theory that specific atrophy patterns are useful in the diagnosis of general AD.

Although cortical atrophy is a well-known marker of neurodegeneration in AD, deep grey matter structure also degenerates. De Jong *et al.* found volumes of the putamen and thalamus were significantly reduced in patients diagnosed with probable Alzheimer's disease and the decrease in volume correlated linearly with impaired global cognitive performance [47]. Research has also found that in early-onset AD, there is a more rapid volumetric decline in the caudate, putamen, and thalamus compared to patients with late onset AD, which is consistent with neuropsychological results [48]. The striatum is affected by AD neuropathology, and pathological studies have revealed early extensive striatal amyloid deposition in PSEN1 mutation carriers [49]. Besides, patients with AD-MCI have lower resting state functional connectivity between the middle striatum and precuneus/cingulate gyrus; this connectivity is negatively correlated with memory performance in AD [50]. The atrophy in subcortical structures, including the caudate, putamen, amygdala and thalamus, was correlated with lower cognitive scores in our study, supporting the utility of considering the subcortical structure in the diagnosis of AD.

We found a significant left predominance in the cognitively relevant cortices either in volume or thickness analysis. Derflinger *et al.* also found grey matter loss in the entorhinal, temporoparietal, dorsofrontal, and occipital cortices as well as in the precuneus in AD patients; however, lobar asymmetry of the temporal, parietal, and occipital lobe with left predominance was observed rather than lateralization [51]. Ossenkoppele *et al.* found the strongest effects of cortical thickness on cognition in the lateral and medial parietal cortex and lateral temporal cortex, while more pronounced in the left temporoparietal cortex for neuropsychological tests evaluating recall and naming [52]. The left predominance of atrophy probably was caused by the right-handedness of most participants and the language-based nature of most cognitive evaluations.

5. LIMITATIONS AND FUTURE DIRECTIONS

This study was not without limitations. Firstly, different cortices were associated with different neuropsychological domains, and domain-specific analysis of cortical atrophy would help the clinical investigation. This analysis is a good direction for future research. Secondly, VBM-based structure was sensitive in the early diagnosis of AD. However, we did not include MCI or prodromal patients in this study. The results support the need to focus further research on community-based populations. Thirdly, the study was cross-sectional, and further longitudinal prospective studies are needed to better evaluate the relationships between cortical atrophy and disease progression. Fourthly, we need to incorporate MRI changes with biomarkers reflecting pathogenesis, such as amyloid and tau PET/CT, which could facilitate the interpretation of the mechanism of brain atrophy.

CONCLUSION

In conclusion, the findings of the study were as follows: (1) The volume of total grey matter was associated with general cognition. (2) Volumes of temporal-parietal-occipital cortex were most significantly correlated with lower cognitive scores evaluated by the MMSE and MoCA; Hippocampus and entorhinal area were also atrophied with worse cognitive performance, but not as strong as the neocortex. (3) Both cortical volume and thickness were sensitive biomarkers of cognitive performance and disease progression in AD. (4) Subcortical grey matter volumes were associated with worse cognitive performance. (5) Cognitively relevant cortices were left predominant. These findings are useful for both clinical and further research and support the use of quantitative structural MRI in the clinical evaluation of cortical changes and specific atrophy patterns in diagnosis and differential diagnosis of AD.

LIST OF ABBREVIATIONS

AD	=	Alzheimer's Disease
MRI	=	Magenatic Resonance Imaging
MMSE	=	Mini-Mental State Examination
MoCA	=	Montreal Cognitive Assessment
ADL	=	Activities of Daily Living
HADS	=	Hospital Anxiety and Depression Scale
FLAIR	=	Fluid-attenuated Inversion Recovery
VBM	=	Voxel Based Morphometry
SBA	=	Surface Based Analysis
MCI	=	Mild Cognitive Impairment
NFTs	=	Neurofibrillary Tangles

ETHICS APPROVAL AND CONSENT TO PARTICIPATE

The ethics committee of Peking Union Medical College Hospital had approved the study, China (No. JS2810).

HUMAN AND ANIMAL RIGHTS

No animals were used in this study. All human procedures were followed in accordance with the guidelines of Declaration of Helsinki 1975.

CONSENT FOR PUBLICATION

All patients or their caregivers were informed regarding the purpose of the study and the publishing of the article. Written consent was obtained from each patient or their caregivers.

STANDARDS OF REPORTING

STROBE guidelines and methodology were followed.

AVAILABILITY OF DATA AND MATERIALS

Not applicable.

FUNDING

This work was supported by the National Key Research and Development Program of China [No. 2020YFA0804500, 2020YFA0804501]; CAMS Innovation Fund for Medical Sciences (CIFMS) (No. 2020-I2M-C&T-B-010, 2021-I2M-1-020); Science Innovation 2030-Brain Science and Brain-Inspired Intelligence Technology Major Project (2021ZD0201106); National Natural Science Foundation of China [No. 81550021, 30470618].

CONFLICT OF INTEREST

The authors declare no conflict of interest, financial or otherwise.

ACKNOWLEDGEMENTS

We would like to thank TopEdit (www.topeditsci.com) for the English language editing of this manuscript.

SUPPLEMENTARY MATERIAL

Supplementary material is available on the publisher's web site along with the published article.

REFERENCES

[1] Blennow K, Leon MJ, Zetterberg H. Alzheimer's disease. Lancet 2006; 368(9533): 387-403. http://dx.doi.org/10.1016/S0140-6736(06)69113-7 PMID: 16876668

[2] Serrano-Pozo A, Frosch MP, Masliah E, Hyman BT. Neuropathological alterations in Alzheimer disease. Cold Spring Harb Perspect Med 2011; 1(1): a006189. http://dx.doi.org/10.1101/cshperspect.a006189 PMID: 22229116

[3] Hardy J, Selkoe DJ. The amyloid hypothesis of Alzheimer's disease: Progress and problems on the road to therapeutics. Science 2002; 297(5580): 353-6. http://dx.doi.org/10.1126/science.1072994 PMID: 12130773

[4] Hampel H, Cummings J, Blennow K, Gao P, Jack CR, Vergallo A. Developing the ATX(N) classification for use across the Alzheimer's disease continuum. Nat Rev Neurol 2021; 17(9): 580-9. http://dx.doi.org/10.1038/s41582-021-00520-w PMID: 34239130

[5] Lane CA, Hardy J, Schott JM. Alzheimer's disease. Eur J Neurol 2018; 25(1): 59-70. http://dx.doi.org/10.1111/ene.13439 PMID: 28872215

[6] Crutch SJ, Lehmann M, Schott JM, Rabinovici GD, Rossor MN, Fox NC. Posterior cortical atrophy. Lancet Neurol 2012; 11(2): 170-8. http://dx.doi.org/10.1016/S1474-4422(11)70289-7 PMID: 22265212

[7] Gorno ML, Hillis AE, Weintraub S, *et al.* Classification of primary progressive aphasia and its variants. Neurology 2011; 76(11): 1006-14. http://dx.doi.org/10.1212/WNL.0b013e31821103e6 PMID: 21325651

[8] Lam B, Masellis M, Freedman M, Stuss DT, Black SE. Clinical, imaging, and pathological heterogeneity of the Alzheimer's disease syndrome. Alzheimers Res Ther 2013; 5(1): 1. http://dx.doi.org/10.1186/alzrt155 PMID: 23302773

[9] McKhann G, Drachman D, Folstein M, Katzman R, Price D, Stadlan EM. Clinical diagnosis of Alzheimer's disease: Report of the NINCDS-ADRDA Work Group* under the auspices of department of health and human services task force on Alzheimer's disease. Neurology 1984; 34(7): 939-44. http://dx.doi.org/10.1212/WNL.34.7.939 PMID: 6610841

[10] McKhann GM, Knopman DS, Chertkow H, *et al.* The diagnosis of dementia due to Alzheimer's disease: Recommendations from the national institute on aging-Alzheimer's association workgroups on

diagnostic guidelines for Alzheimer's disease. Alzheimers Dement 2011; 7(3): 263-9.
http://dx.doi.org/10.1016/j.jalz.2011.03.005 PMID: 21514250

[11] Kunst J, Marecek R, Klobusiakova P, *et al.* Patterns of grey matter atrophy at different stages of Parkinson's and Alzheimer's diseases and relation to cognition. Brain Topogr 2019; 32(1): 142-60.
http://dx.doi.org/10.1007/s10548-018-0675-2 PMID: 30206799

[12] Risacher S, Saykin A, Wes J, Shen L, Firpi H, McDonald B. Baseline MRI predictors of conversion from MCI to probable AD in the ADNI cohort. Curr Alzheimer Res 2009; 6(4): 347-61.
http://dx.doi.org/10.2174/156720509788929273 PMID: 19689234

[13] Scheltens P, Leys D, Barkhof F, *et al.* Atrophy of medial temporal lobes on MRI in "probable" Alzheimer's disease and normal ageing: Diagnostic value and neuropsychological correlates. J Neurol Neurosurg Psychiatry 1992; 55(10): 967-72.
http://dx.doi.org/10.1136/jnnp.55.10.967 PMID: 1431963

[14] Koedam ELGE, Lehmann M, van der Flier WM, *et al.* Visual assessment of posterior atrophy development of a MRI rating scale. Eur Radiol 2011; 21(12): 2618-25.
http://dx.doi.org/10.1007/s00330-011-2205-4 PMID: 21805370

[15] Jang JW, Park SY, Park YH, *et al.* A comprehensive visual rating scale of brain magnetic resonance imaging: Application in elderly subjects with Alzheimer's disease, mild cognitive impairment, and normal cognition. J Alzheimers Dis 2015; 44(3): 1023-34.
http://dx.doi.org/10.3233/JAD-142088 PMID: 25380589

[16] Jack CR Jr, Bennett DA, Blennow K, *et al.* NIA-AA research framework: Toward a biological definition of Alzheimer's disease. Alzheimers Dement 2018; 14(4): 535-62.
http://dx.doi.org/10.1016/j.jalz.2018.02.018 PMID: 29653606

[17] Mao C, Li J, Huang X, *et al.* White matter hyperintensities and patterns of atrophy in early onset Alzheimer's disease with causative gene mutations. Clin Neurol Neurosurg 2021; 203: 106552.
http://dx.doi.org/10.1016/j.clineuro.2021.106552 PMID: 33601235

[18] Scahill RI, Ridgway GR, Bartlett JW, *et al.* Genetic influences on atrophy patterns in familial Alzheimer's disease: A comparison of APP and PSEN1 mutations. J Alzheimers Dis 2013; 35(1): 199-212.
http://dx.doi.org/10.3233/JAD-121255 PMID: 23380992

[19] Sławek J, Narożańska E, Brockhuis B, *et al.* Neuroimaging in the differential diagnosis of primary progressive aphasia - illustrative case series in the light of new diagnostic criteria. Pol Przegl Radiol Med Nukl 2014; 79: 251-8.
http://dx.doi.org/10.12659/PJR.890320 PMID: 25343001

[20] Whitwell JL, Jack CR Jr, Kantarci K, *et al.* Imaging correlates of posterior cortical atrophy. Neurobiol Aging 2007; 28(7): 1051-61.
http://dx.doi.org/10.1016/j.neurobiolaging.2006.05.026 PMID: 16797786

[21] Ashburner J, Csernansk JG, Davatzikos C, Fox NC, Frisoni GB, Thompson PM. Computer-assisted imaging to assess brain structure in healthy and diseased brains. Lancet Neurol 2003; 2(2): 79-88.
http://dx.doi.org/10.1016/S1474-4422(03)00304-1 PMID: 12849264

[22] Fischl B, Salat DH, Busa E, *et al.* Whole brain segmentation: Automated labeling of neuroanatomical structures in the human brain. Neuron 2002; 33(3): 341-55.
http://dx.doi.org/10.1016/S0896-6273(02)00569-X PMID: 11832223

[23] Fennema NC, Hagler DJ Jr, McEvoy LK, *et al.* Structural MRI biomarkers for preclinical and mild Alzheimer's disease. Hum Brain Mapp 2009; 30(10): 3238-53.
http://dx.doi.org/10.1002/hbm.20744 PMID: 19277975

[24] Dickerson BC, Bakkour A, Salat DH, *et al.* The cortical signature of Alzheimer's disease: Regionally specific cortical thinning relates to symptom severity in very mild to mild AD dementia and is detectable in asymptomatic amyloid-positive individuals. Cereb Cortex 2009; 19(3): 497-510.
http://dx.doi.org/10.1093/cercor/bhn113 PMID: 18632739

[25] McDonald CR, McEvoy LK, Gharapetian L, *et al.* Regional rates of neocortical atrophy from normal aging to early Alzheimer's disease. Neurology 2009; 73(6): 457-65.
http://dx.doi.org/10.1212/WNL.0b013e3181b16431 PMID: 19667321

[26] McEvoy LK, Brewer JB. Quantitative structural MRI for early detection of Alzheimer's disease. Expert Rev Neurother 2010; 10(11): 1675-88.
http://dx.doi.org/10.1586/ern.10.162 PMID: 20977326

[27] Mao C, Sha L, Li J, *et al.* Relationship between general cognition, visual assessed cortical atrophy, and cerebrospinal fluid biomarkers in Alzheimer's disease: A cross sectional study from a Chinese PUMCH Cohort. J Alzheimers Dis 2021; 82(1): 205-14.
http://dx.doi.org/10.3233/JAD-210344 PMID: 34024840

[28] Tan J, Li N, Gao J, *et al.* Optimal cutoff scores for dementia and mild cognitive impairment of the Montreal Cognitive Assessment among elderly and oldest-old Chinese population. J Alzheimers Dis 2014; 43(4): 1403-12.
http://dx.doi.org/10.3233/JAD-141278 PMID: 25147113

[29] Ashburner J, Friston KJ. Voxel based morphometry the methods. Neuroimage 2000; 11(6): 805-21.
http://dx.doi.org/10.1006/nimg.2000.0582 PMID: 10860804

[30] Whitwell JL. Voxel based morphometry: An automated technique for assessing structural changes in the brain. J Neurosci 2009; 29(31): 9661-4.
http://dx.doi.org/10.1523/JNEUROSCI.2160-09.2009 PMID: 19657018

[31] Meyer P, Feldkamp H, Hoppstädter M, *et al.* Using voxel-based morphometry to examine the relationship between regional brain volumes and memory performance in amnestic mild cognitive impairment. Front Behav Neurosci 2013; 7: 89.
http://dx.doi.org/10.3389/fnbeh.2013.00089 PMID: 23888131

[32] Tabatabaei JH, Shaw ME, Walsh E, Cherbuin N. Regional brain atrophy predicts time to conversion to Alzheimer's disease, dependent on baseline volume. Neurobiol Aging 2019; 83: 86-94.
http://dx.doi.org/10.1016/j.neurobiolaging.2019.08.033 PMID: 31585370

[33] Poulakis K, Pereira JB, Mecocci P, *et al.* Heterogeneous patterns of brain atrophy in Alzheimer's disease. Neurobiol Aging 2018; 65: 98-108.
http://dx.doi.org/10.1016/j.neurobiolaging.2018.01.009 PMID: 29455029

[34] Risacher SL, Anderson WH, Charil A, *et al.* Alzheimer disease brain atrophy subtypes are associated with cognition and rate of decline. Neurology 2017; 89(21): 2176-86.
http://dx.doi.org/10.1212/WNL.0000000000004670 PMID: 29070667

[35] Kate M, Dicks E, Visser PJ, *et al.* Atrophy subtypes in prodromal Alzheimer's disease are associated with cognitive decline. Brain 2018; 141(12): 3443-56.
http://dx.doi.org/10.1093/brain/awy264 PMID: 30351346

[36] Möller C, Vrenken H, Jiskoot L, *et al.* Different patterns of gray matter atrophy in early- and late-onset Alzheimer's disease. Neurobiol Aging 2013; 34(8): 2014-22.
http://dx.doi.org/10.1016/j.neurobiolaging.2013.02.013 PMID: 23561509

[37] Shima K, Matsunari I, Samuraki M, *et al.* Posterior cingulate atrophy and metabolic decline in early stage Alzheimer's disease. Neurobiol Aging 2012; 33(9): 2006-17.
http://dx.doi.org/10.1016/j.neurobiolaging.2011.07.009 PMID: 21855172

[38] Kilimann I, Grothe M, Heinsen H, *et al.* Subregional basal forebrain atrophy in Alzheimer's disease: A multicenter study. J Alzheimers Dis 2014; 40(3): 687-700.
http://dx.doi.org/10.3233/JAD-132345 PMID: 24503619

[39] Sabuncu MR, Desikan RS, Sepulcre J, *et al.* The dynamics of cortical and hippocampal atrophy in Alzheimer disease. Arch Neurol 2011; 68(8): 1040-8.
http://dx.doi.org/10.1001/archneurol.2011.167 PMID: 21825241

[40] Lee JS, Park YH, Park S, *et al.* Distinct brain regions in physiological and pathological brain aging. Front Aging Neurosci 2019; 11: 147.
http://dx.doi.org/10.3389/fnagi.2019.00147 PMID: 31275140

[41] Velayudhan L, Proitsi P, Westman E, *et al.* Entorhinal cortex thickness predicts cognitive decline in Alzheimer's disease. J Alzheimers Dis 2013; 33(3): 755-66.
http://dx.doi.org/10.3233/JAD-2012-121408 PMID: 23047370

[42] Gómez IT, Hollister R, West H, *et al.* Neuronal loss correlates with but exceeds neurofibrillary tangles in Alzheimer's disease. Ann Neurol 1997; 41(1): 17-24. http://dx.doi.org/10.1002/ana.410410106 PMID: 9005861

[43] Braak H, Alafuzoff I, Arzberger T, Kretzschmar H, Del Tredici K. Staging of Alzheimer disease-associated neurofibrillary pathology using paraffin sections and immunocytochemistry. Acta Neuropathol 2006; 112(4): 389-404. http://dx.doi.org/10.1007/s00401-006-0127-z PMID: 16906426

[44] Giannakopoulos P, Bouras C, Hof PR. Alzheimer's disease with asymmetric atrophy of the cerebral hemispheres: Morphometric analysis of four cases. Acta Neuropathol 1994; 88(5): 440-7. http://dx.doi.org/10.1007/BF00389496 PMID: 7847073

[45] Murray ME, Graff RNR, Ross OA, Petersen RC, Duara R, Dickson DW. Neuropathologically defined subtypes of Alzheimer's disease with distinct clinical characteristics: A retrospective study. Lancet Neurol 2011; 10(9): 785-96. http://dx.doi.org/10.1016/S1474-4422(11)70156-9 PMID: 21802369

[46] Whitwell JL, Jack CR Jr, Przybelski SA, *et al.* Temporoparietal atrophy: A marker of AD pathology independent of clinical diagnosis. Neurobiol Aging 2011; 32(9): 1531-41. http://dx.doi.org/10.1016/j.neurobiolaging.2009.10.012 PMID: 19914744

[47] Jong LW, Hiele K, Veer IM, *et al.* Strongly reduced volumes of putamen and thalamus in Alzheimer's disease: An MRI study. Brain 2008; 131(12): 3277-85. http://dx.doi.org/10.1093/brain/awn278 PMID: 19022861

[48] Cho H, Seo SW, Kim JH, *et al.* Changes in subcortical structures in early- *versus* late-onset Alzheimer's disease. Neurobiol Aging 2013; 34(7): 1740-7. http://dx.doi.org/10.1016/j.neurobiolaging.2013.01.001 PMID: 23394958

[49] Klunk WE, Price JC, Mathis CA, *et al.* Amyloid deposition begins in the striatum of presenilin-1 mutation carriers from two unrelated pedigrees. J Neurosci 2007; 27(23): 6174-84. http://dx.doi.org/10.1523/JNEUROSCI.0730-07.2007 PMID: 17553989

[50] Anderkova L, Barton M, Rektorova I. Striato cortical connections in Parkinson's and Alzheimer's diseases: Relation to cognition. Mov Disord 2017; 32(6): 917-22. http://dx.doi.org/10.1002/mds.26956 PMID: 28256044

[51] Derflinger S, Sorg C, Gaser C, *et al.* Grey matter atrophy in Alzheimer's disease is asymmetric but not lateralized. J Alzheimers Dis 2011; 25(2): 347-57. http://dx.doi.org/10.3233/JAD-2011-110041 PMID: 21422522

[52] Ossenkoppele R, Smith R, Ohlsson T, *et al.* Associations between tau, Aβ, and cortical thickness with cognition in Alzheimer's disease. Neurology 2019; 92(6): e601-12. http://dx.doi.org/10.1212/WNL.0000000000006875 PMID: 30626656